A General Conformal-Mapping Approach to the Optimum Electrode Design of Coplanar Waveguides With Arbitrary Cross Section

Michele Goano, *Member, IEEE*, Francesco Bertazzi, Paolo Caravelli, Giovanni Ghione, *Senior Member, IEEE*, and Tobin A. Driscoll

***Abstract*—The *Schwarz–Christoffel toolbox*, a free MATLAB package for the computation of conformal maps, is applied to the quasi-static analysis of coplanar waveguides (CPWs) of arbitrary cross section in order to provide computationally efficient and very accurate estimates of their capacitance, inductance, characteristic impedance, and skin-effect attenuation. A few examples of many-sided polygonal waveguides are discussed, and the trapezoidal CPW, important, for example, for electrooptic modulators, is described in full detail, providing general guidelines for the electrode geometry optimization. The technique is validated through a comparison with the results of a full-wave finite-element method, and excellent agreement is demonstrated both *in vacuo* and with two-layer dielectric substrates.**

***Index Terms*—Coplanar waveguides, electrooptic modulation, integrated opto-electronics, skin effect.**

I. Introduction

CONFORMAL mapping (CM) plays an important role among the techniques used in the study of microwave transmission lines in quasi-static approximation. This method directly enables the exact evaluation of the *in vacuo* line capacitance and, therefore, the line inductance and characteristic impedance; the skin-effect line resistance can also be exactly evaluated, while suitable approximations can often be provided to the line capacitance and conductance in the presence of a dielectric substrate.

The Schwarz–Christoffel (SC) formula, a special conformal transformation devised for polygonal regions (see, e.g., [1]–[3]), has been widely applied to coaxial structures, strip lines, and coplanar waveguides (CPWs) in order to get closed-form expressions for the line characteristic parameters, usually in terms of complete elliptic integrals ([4, Sec. 6.1]). This "analytical" application of the SC mapping is limited to rather simple line cross sections with zero-thickness electrodes (see, e.g., [5] and [6]). More recently, growing interest in monolithic microwave integrated circuits (MMICs) and electrooptic devices requiring thick-electrode waveguides (i.e., having electrode thickness comparable with the width of the central line and/or the gap between line and ground planes) has led to *ad hoc* solutions for finite-thickness rectangular CPWs, both in terms of accurate analytical approximations [7] and of numerical inversion of the SC transformation [8], [9].

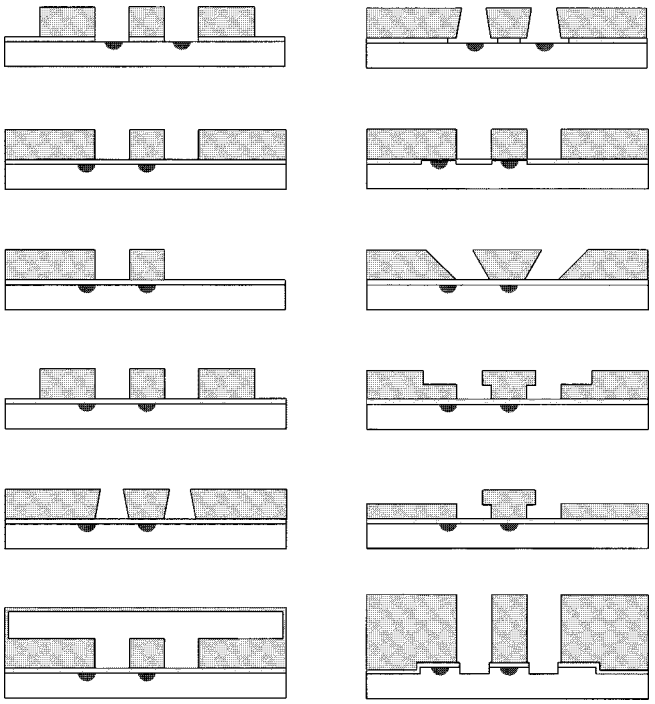

Fig. 1. Cross sections of high-performance $LiNbO_3$ electrooptical modulator structures on X-cut (top line) and Z-cut substrates. The diffused optical waveguides are dark grey. A thin SiO_2 layer (light grey) is interposed between the substrate and thick gold electrodes.

To date, one of the most challenging problems where SC transformation may become an important design tool is the optimization of the electrode geometry in $LiNbO_3$ electrooptical modulators. In this class of devices, loss minimization is essential in order to achieve high modulation bandwidths (>40 GHz), and losses are mainly determined by the electrodes cross section. The effect of different geometries has been investigated in several laboratories in the last decade (see, e.g., [10]–[13]): a few examples of high-performance modulator structures are reported in Fig. 1. No general quantitative design criteria for loss minimization are available yet, apart from the evidence of the advantages of thick metallizations. Even the thick rectangular SC mappings [7]–[9] are unable to cope with most of the geometries proposed thus far and, at present, the main analysis tools

Manuscript received October 13, 2000. This work was supported in part by the Consiglio Nazionale delle Ricerche under the MADESS II Project. The work of F. Bertazzi was supported by Pirelli Optical Components under a grant.

M. Goano, F. Bertazzi, P. Caravelli, and G. Ghione are with the Dipartimento di Elettronica, Politecnico di Torino, I-10129 Turin, Italy (e-mail: goano@polito.it).

T. A. Driscoll is with the Department of Mathematical Sciences, University of Delaware, Newark, DE 19716 USA (e-mail: driscoll@math.udel.edu).

Publisher Item Identifier S 0018-9480(01)07582-2.

are the quasi-static finite-element method (QS FEM) [13]–[15] and full-wave finite-element method (FW FEM) [16]. Unfortunately, the QS FEM cannot reliably evaluate conductor losses (the numerical implementation of Wheeler's incremental inductance rule [17] can lead to inaccurate results because of field singularities), and the FW FEM is usually too computationally expensive to allow a detailed exploration of the design's parameter space, and is also affected by numerical problems in the evaluation of losses because of the singular current distribution at the edges of the conductors.

This paper introduces a generalized CM approach to the design of (symmetrical) CPW electrodes of arbitrary polygonal geometry based on the robust and efficient numerical solutions provided by the SC toolbox [18], [19], a collection of MATLAB[1] functions for the interactive computation and visualization of SC conformal maps.[2] The approach is *exact* insofar as the quasi-static *in vacuo* capacitance, inductance, and characteristic impedance are concerned. Skin-effect losses are computed exactly from the high-frequency current density distribution, through an extension of the method first proposed in [20] and subsequently applied to thin [21]–[25] and thick [8], [9] rectangular CPWs. A simple partial capacitance approach [9] is exploited to approximate the effective dielectric constant $\epsilon_{\rm eff}$, thus enabling the study of CPWs on one- or two-layer substrates, such as SiO_2-coated $LiNbO_3$. More complex dielectric geometries may be considered by coupling CM with a QS FEM simulator, much simpler and faster than an FW FEM.

The paper is organized as follows. Section II presents the complete discussion of a relevant case study, i.e., the trapezoidal CPW. In order to help the reader, all the conformal transformations involved are shown both analytically and graphically, and the detailed recipes for the computation of all the waveguide parameters with the SC toolbox are given. The model is validated through a comparison with the FW FEM, and a simple example of graphical optimization of the line cross section is provided. The application of our tool to waveguides with general polygonal geometry is described in Section III. Finally, the present limitations and future extensions of the model are discussed.

II. Case Study—Trapezoidal CPW

In order to demonstrate the potential of the SC toolbox applied to the modeling of microwave guides, we will discuss in detail a simple yet important example, i.e., the trapezoidal CPW. The exploitation of nonrectangular geometries in order to improve electrooptic modulator performances has been investigated in [26] and [27], and thick trapezoidal electrodes have been used in [13] and [26]. To our knowledge, CM techniques have been applied to thick trapezoidal structures only in [8], but the resulting *ad hoc* implementation of the parameter problem required careful user intervention in order to overcome the instabilities deriving from the lack of good initial guesses.

Fig. 2(a) shows the cross section of a generic symmetric trapezoidal CPW with infinite-width ground planes, described by six geometric parameters ($a, b, t_l, t_g, \beta_l, \beta_g$, where angles β_l, β_g are positive for over-cut electrodes). The half-structure

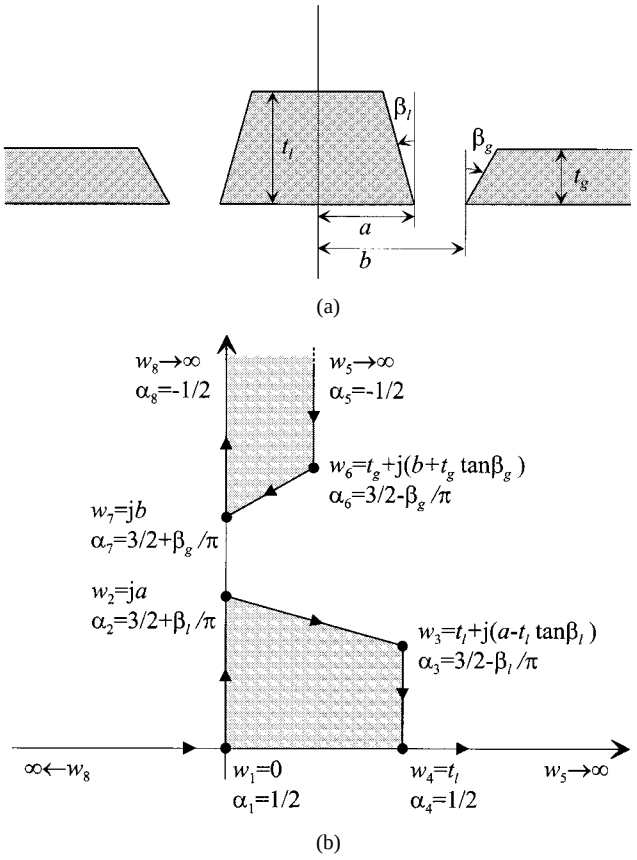

Fig. 2. Cross section of a trapezoidal CPW and parametric representation of the corresponding polygon in the physical domain. The coordinates of the vertices w_i and the interior angles at the vertices $\pi\alpha_i$ are reported.

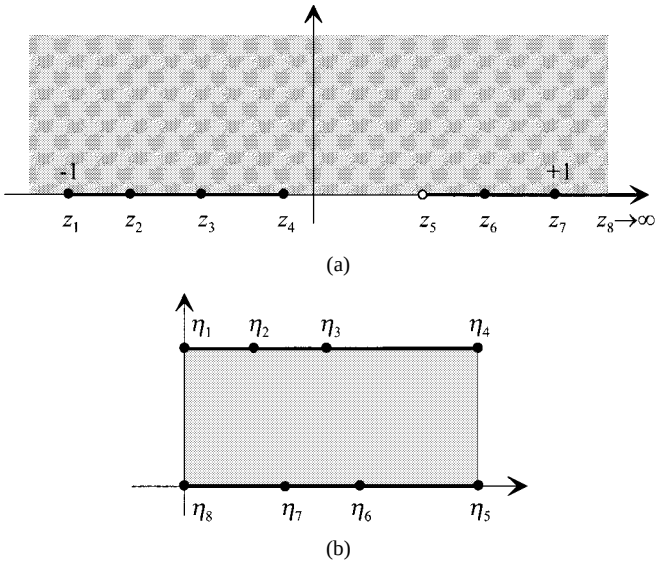

Fig. 3. Mapping of the trapezoidal CPW into the canonical plane and final transformation into a rectangular region (parallel-plate capacitor).

drawn in Fig. 2(b) is a simply connected polygon with two infinite vertices. For each vertex, the coordinates $w_1, \ldots, w_8$ and the corresponding interior angles $\pi\alpha_1, \ldots, \pi\alpha_8$ are reported, expressed in terms of the geometric parameters of the line. The polygon in the physical domain may be transformed in the upper half-plane [the canonical domain, shown in Fig. 3(a)] by means

[1]MATLAB is a registered trademark of The MathWorks Inc., Natick, MA.

[2][Online]. Available: http://www.math.udel.edu/~driscoll/software/

of the SC mapping shown in (1), at the bottom of this page, where $\mathcal{K}$ is a complex constant, and three prevertices may be chosen arbitrarily (the SC toolbox imposes $z_1 = -1, z_7 = +1$, and $z_8 \to \infty$), thus yielding a parameter problem with five unknowns. The determination of these real numbers requires the solution of a system of five nonlinear equations, involving the computation of seven hyperelliptic integrals whose singular end points are the unknown prevertices. An additional problem is represented by the nonintegratable singularity in z_5, which must be avoided by choosing an integration path in the complex plane. The function `hplmap` of the SC toolbox provides an accurate solution of the parameter problem, computing the constant $\mathcal{K}$ and the prevertices $z_2, \ldots, z_6$ as a function of the vectors $\{w_i\}$ and $\{\alpha_i\}$. Eventually, the strips in the canonical domain are transformed via an inverse closed-form SC mapping into the parallel plates of a rectangular capacitor [see Fig. 3(b)]. Therefore, the exact quasi-static *in vacuo* per-unit-length capacitance, per-unit-length inductance, and characteristic impedance of the CPW may be computed as[3]

$$C_0 = 2\epsilon_0 \frac{|\eta_4 - \eta_1|}{|\eta_4 - \eta_5|} = 2\epsilon_0 \frac{K(k)}{K(k')} \tag{2}$$

$$L_0 = \frac{1}{c^2 C_0} \tag{3}$$

$$Z_0 = \frac{1}{cC_0} \tag{4}$$

where c is the speed of light in vacuum, $\epsilon_0 = 1/\mu_0 c^2, \mu_0 = 4\pi \cdot 10^7$ H/m, $K(k)$ is the complete elliptic integral of the first kind, $k' = \sqrt{1-k^2}$, and

$$k = \sqrt{\frac{z_4 - z_1}{z_5 - z_1}}. \tag{5}$$

The *in vacuo* skin-effect per-unit-length attenuation may be approximated with a high degree of accuracy by the conventional expression

$$\alpha_0 = \frac{R_s}{2Z_0 I_{\text{line}}^2} \oint_\gamma |J|^2 \, dl \tag{6}$$

where $R_s = 1/\sigma\delta(f)$ is the skin-effect surface resistance of the metallic conductors, $\delta(f) = 1/\sqrt{\pi f \mu_0 \sigma}$ is the frequency-dependent skin-effect current penetration depth, σ is the metal conductivity, I_{line} is the total current carried by the central line, and J is the surface current density, defined over all the CPW periphery γ. I_{line} may be immediately computed as

$$\begin{aligned} I_{\text{line}} &= \int_{\text{line}} |J(w)| \, dw = 2\mathcal{I} \int_{z_1}^{z_4} \left| \frac{d\eta}{dz} \right| dz \\ &= 2\mathcal{I} \int_{z_1}^{z_4} \left| \frac{1}{\sqrt{(z-z_1)(z-z_4)(z-z_5)}} \right| dz \\ &= 4\mathcal{I} \frac{K(k)}{\sqrt{z_5 - z_1}} \end{aligned} \tag{7}$$

where $\mathcal{I}$ is a scale factor representing the uniform current density in the η-plane. The integration of $|J|^2$ is performed in the canonical domain

$$\oint_\gamma |J|^2 \, dl = 2\mathcal{I}^2 \int_{\gamma_z} \left| \frac{d\eta}{dz} \right|^2 \left| \frac{dz}{dw} \right| dz = \frac{2\mathcal{I}^2}{\mathcal{K}} \int_{\gamma_z} |P(z)| \, dz \tag{8}$$

where

$$\begin{aligned} P(z) &= (z-z_1)^{-1/2}(z-z_2)^{-1/2-\beta_l/\pi}(z-z_3)^{-1/2+\beta_l/\pi} \\ &\quad \times (z-z_4)^{-1/2}(z-z_5)^{1/2}(z-z_6)^{-1/2+\beta_g/\pi} \\ &\quad \times (z-z_7)^{-1/2-\beta_g/\pi} \\ &= \prod_{i=1}^{7} (z-z_i)^{\theta_i - 1} \end{aligned} \tag{9}$$

and γ_z is the half-structure contour mapped on the real axis of the z-plane

$$\begin{aligned} \gamma_z = (z_1, z_2) \cup (z_2, z_3) \cup (z_3, z_4) \\ \cup [z_5, z_6) \cup (z_6, z_7) \cup (z_7, \infty). \end{aligned} \tag{10}$$

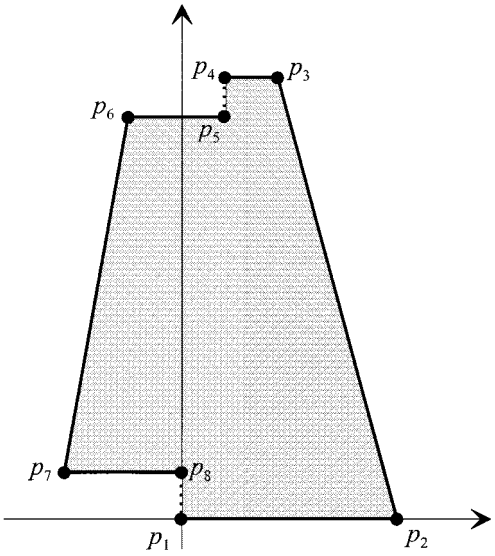

Fig. 4. Bounded polygon whose vertices $p_1, \ldots, p_8$ are mapped into the prevertices $z_1, \ldots, z_8$ [see Fig. 3(a)] by the SC transformation defined by $P(z)$. The length of each side of the polygon is proportional to the integral of $|J|^2$ on the corresponding side of the CPW in the canonical domain [see Fig. 2(b)].

[3]The transformation from the upper half-plane to the parallel-plate capacitor can be easily solved by the SC toolbox, with no need of invoking the complete elliptic integrals, but we have preferred to retain an expression that may look familiar to most microwave engineers. However, it must be remembered that, unlike the numerical solution provided by the SC toolbox, the computation of the ratio of complete elliptic integrals may be affected by severe inaccuracies for $k \approx 0$ or $k \approx 1$ if good asymptotic approximations [28] are not used.

$$\frac{dw}{dz} = \mathcal{K} \prod_{i=1}^{7} (z-z_i)^{\alpha_i - 1} = \mathcal{K} \frac{(z-z_2)^{1/2+\beta_l/\pi}(z-z_3)^{1/2-\beta_l/\pi}(z-z_6)^{1/2-\beta_g/\pi}(z-z_7)^{1/2+\beta_g/\pi}}{\sqrt{z-z_1}\sqrt{z-z_4}(z-z_5)^{3/2}} \tag{1}$$

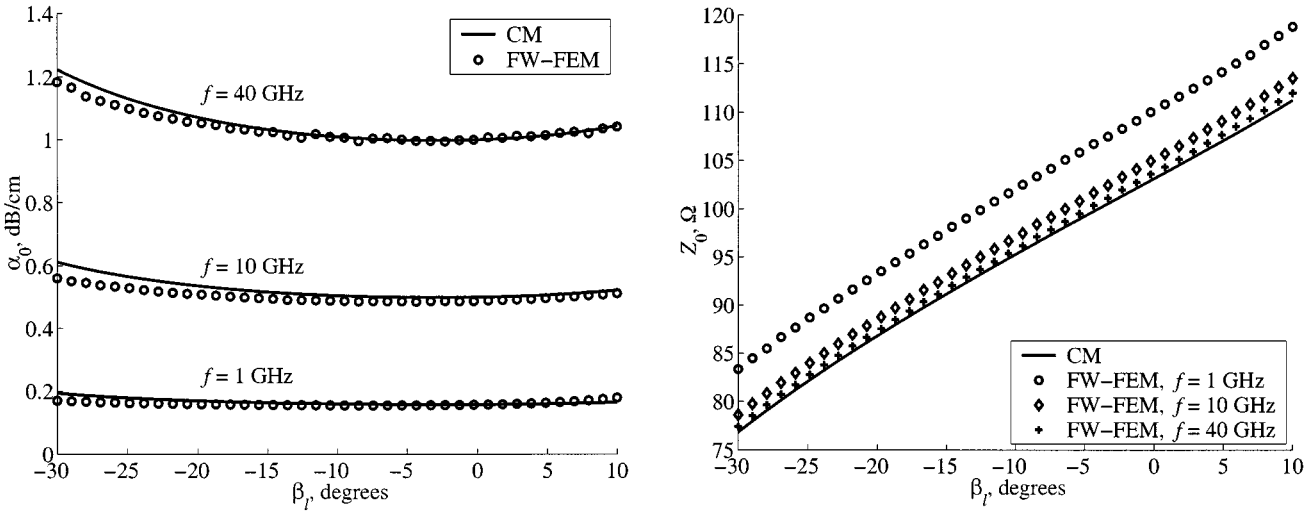

Fig. 5. Comparison between attenuation (in decibels per centimeter) and characteristic impedance (Ω) of a trapezoidal CPW *in vacuo* ($a = 4\ \mu$m, $b = 24\ \mu$m, $t_l = t_g = 15\ \mu$m, $\beta_g = 0°$) computed with the FW FEM and with the present approach at $f = 1, 10, 40$ GHz, as a function of the edges inclination of the central electrode β_l.

The integrals on these six intervals could be computed by applying the same numerical tools used in [8] (the Fortran routines `QAGI` and `QAGS` of the QUADPACK library[4] [29] are at the core of the MATLAB functions `d01apf` and `d01amf` of the NAG Foundation toolbox). However, the simplest and most computationally efficient approach is to notice that $P(z)$ is simply another SC integrand. In the corresponding transformation, the prevertices $z_1, \ldots, z_8$ are the images of the vertices $p_1, \ldots, p_8$ of the bounded region represented in Fig. 4. Given the prevertices $z_1, \ldots, z_8$ and the angles $\theta_1, \ldots, \theta_8$, the function `hplmap` will evaluate all the integrals in (8), thus providing the coordinates of the vertices $p_1, \ldots, p_8$. From a geometrical standpoint, the integral of $|P(z)|$ is the perimeter of the polygon defined by $\{p_i\}$ (with the exception of its two vertical sides); therefore, the problem of minimizing the line losses, given suitable constraints on the line geometry, can be translated into a geometrical perimeter minimization problem.

In the study of "pathological" structures (where, e.g., line and ground planes are almost overlapping), the numerical convergence of the standard SC transformation implemented in `hplmap` may be hampered by a severe crowding of the prevertices. This phenomenon can usually be prevented by choosing as canonical domain a rectangle instead of the upper half-plane, therefore, mapping the CPW directly into a parallel-plate capacitor. In the SC toolbox, instead of `hplmap`, this is done by using the function `rectmap` (or `crrectmap` in extreme cases of bad conditioning [30]).

The effect of a planar substrate on the characteristic parameters may be accurately approximated by a partial capacitance approach [9]

$$C_c = (C_0 - C_{\text{thin}}/2) + C_{\text{llp}} \tag{11}$$

$$Z_c = 1\Big/\left(c\sqrt{C_c C_0}\right) \tag{12}$$

$$\alpha_c = \sqrt{\epsilon_{\text{eff}}}\,\alpha_0 \tag{13}$$

where $\epsilon_{\text{eff}} = C_c/C_0$, C_{thin} is the *in vacuo* per-unit-length capacitance of a zero-thickness CPW having the same dimensions a, b of the thick trapezoidal CPW, and C_{llp} is the per-unit-length capacitance of the lower half-plane. For bulk substrates, C_{llp} may be computed following [7]. Two-layer substrates (like the SiO_2-coated $LiNbO_3$ wafers commonly used in electrooptical modulators) may be described with the approach proposed in [9]. Future work will extend our tool to arbitrarily complex substrates (e.g., including ridges and/or several lossy dielectric layers, also with electrodes laying on different planes), by coupling CM with QS FEM.

The CM results have been validated through a comparison with our MATLAB implementation of FW FEM based on [16], [31]–[35]. The application of Galerkin's procedure to the vector wave equation, with the use of hybrid triangular edge/nodal elements, gives a generalized eigensystem to solve for propagation constants directly, and avoids the occurrence of spurious modes. The sparse eigenvalue problem is solved with the function `sptarn` of the MATLAB partial differential equations (PDEs) toolbox, based on the implicitly restarted Arnoldi method [36] as implemented in ARPACK [37].[5] Figs. 5 and 6 show the attenuation and characteristic impedance of a trapezoidal CPW, *in vacuo* and on an $SiO_2/LiNbO_3$ substrate, computed with the present CM approach and with the FW FEM (in all the simulations presented in this paper, we used $\sigma = 4.1 \cdot 10^7$ S/m). It may be observed that the agreement between the attenuations is always very satisfying and, as expected, the FW FEM characteristic impedance becomes virtually coincident with the quasi-static CM value at high frequency. It is important to note that, on a PC with a 600-MHz CPU, the computation of one curve of Figs. 5 and 6 (40 samples) takes about 13 s with CM, and about 2400 s with the FW FEM (which rebuilds a new mesh for every value of β_l).

As a simple example of the use of our general CM approach as an optimization tool, Figs. 7 and 8 show maps of the attenuation and characteristic impedance at $f = 1$ GHz of a trapezoidal

[4][Online]. Available: http://www.netlib.org/quadpack

[5][Online]. Available: http://www.caam.rice.edu/software/ARPACK/

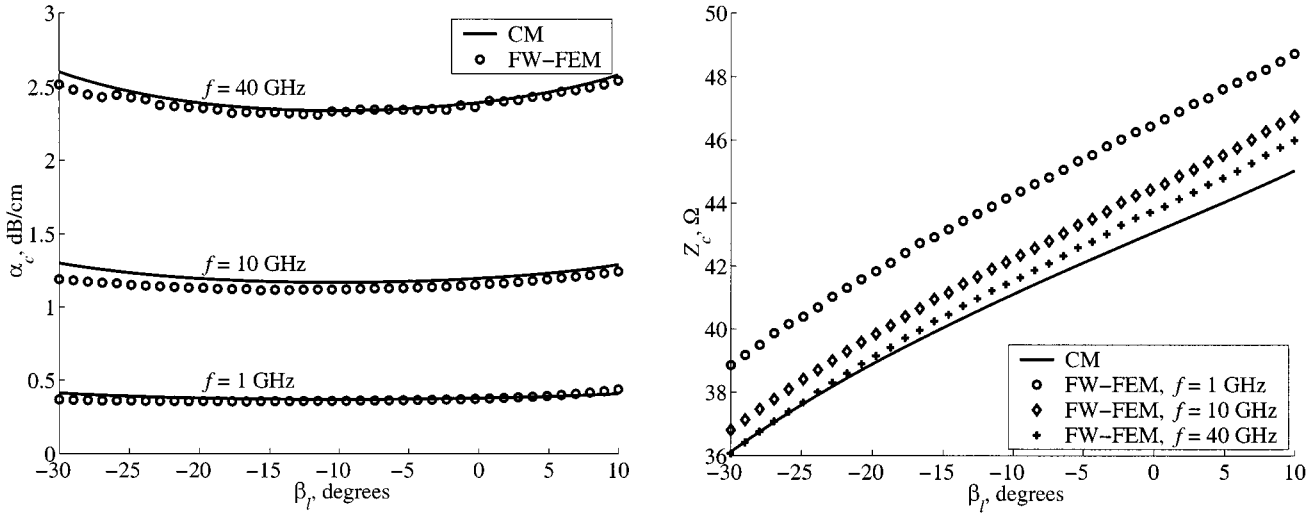

Fig. 6. Comparison between attenuation (in decibels per centimeter) and characteristic impedance (Ω) of a trapezoidal CPW ($a = 4\ \mu$m, $b = 24\ \mu$m, $t_l = t_g = 15\ \mu$m, $\beta_g = 0°$) on an $LiNbO_3$ substrate with a 1-μm-thick SiO_2 buffer ($\epsilon_r = 3.90$), computed with the FW FEM and with the present approach at $f = 1, 10, 40$ GHz as a function of the edges inclination of the central electrode β_l. For $LiNbO_3$, CM uses the equivalent quasi-static isotropic relative dielectric permittivity ([40, Eq. (63)]) $\epsilon_{r,\mathrm{eq}} = \sqrt{\epsilon_{11}\epsilon_{33}} = 34.70$, while the anisotropic FW FEM uses the components of the permittivity tensor ($\epsilon_{11} = 28, \epsilon_{33} = 43$). Losses in $LiNbO_3$ and SiO_2 have been neglected.

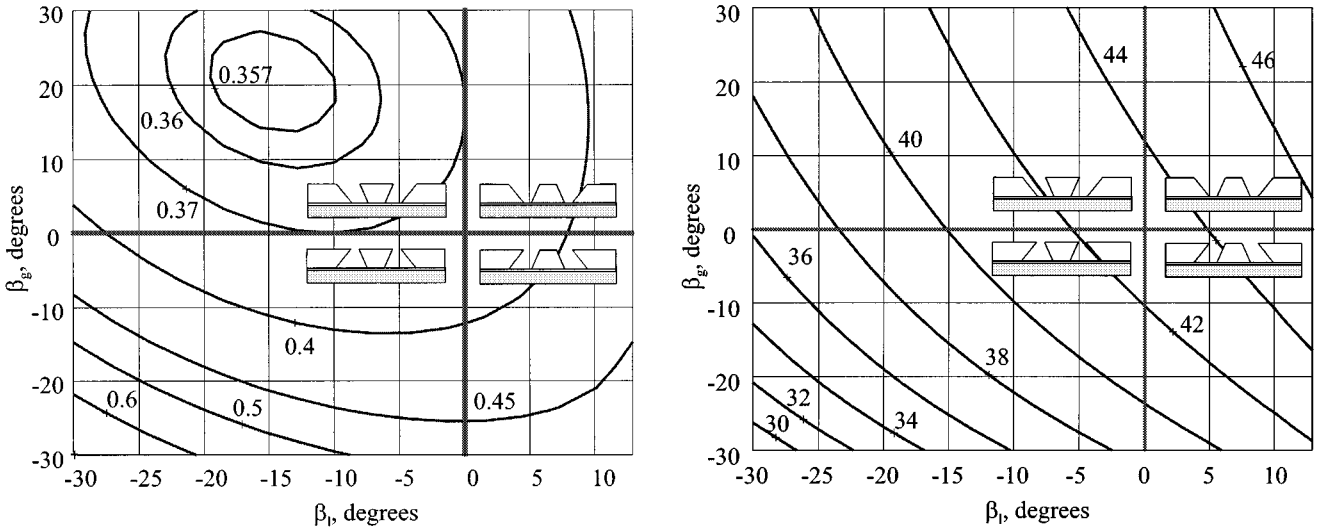

Fig. 7. Attenuation (in decibels per centimeter) and characteristic impedance (Ω) at $f = 1$ GHz of a trapezoidal CPW ($a = 4\ \mu$m, $b = 24\ \mu$m, $t_l = t_g = 15\ \mu$m) as a function of the edges inclination of central electrode and ground planes β_l, β_g. The substrate is the same as in Fig. 6.

CPW on an $LiNbO_3$ substrate with an SiO_2 buffer as functions of β_l, β_g, and t_l. Using uniformly thick electrodes ($t_l = t_g$, Fig. 7), it may be observed that the minimum-loss electrode shape occurs with an overcutting of the central electrode and an undercutting of the ground planes, thus confirming the suggestion in [12]; the corresponding impedance level is around 40 Ω, which is acceptable for modulator applications. The optimum geometrical shape is difficult to directly obtain through electroplating, although it can be approximated by multilevel metallizations [12]. Fig. 8 concerns another optimization exercise, where the effects of the central electrode thickness and shape are explored. As expected, the attenuation heavily depends on the central line thickness, while further improvements may be produced by a slight overcutting of the central electrode. In practice, this could be obtained through electroplating with a properly cured photoresist. Apart from technological limitations, increasing the electrode thickness leads to a less favorable impedance level.

III. General Case

The approach described for the complete characterization of trapezoidal CPWs may be extended in a straightforward way to CPWs with arbitrary polygonal cross section and infinite-width ground planes; in its present form, the application of the method requires certain symmetries to be present, as discussed in detail at the conclusion of this section.

Let us consider a general symmetrical CPW, completely defined by half of the structure. The (half) central electrode is described by n_l vertices, while the ground plane is described by n_g vertices (including two vertices at infinity). To carry out the line analysis, one has simply to provide the SC toolbox with the

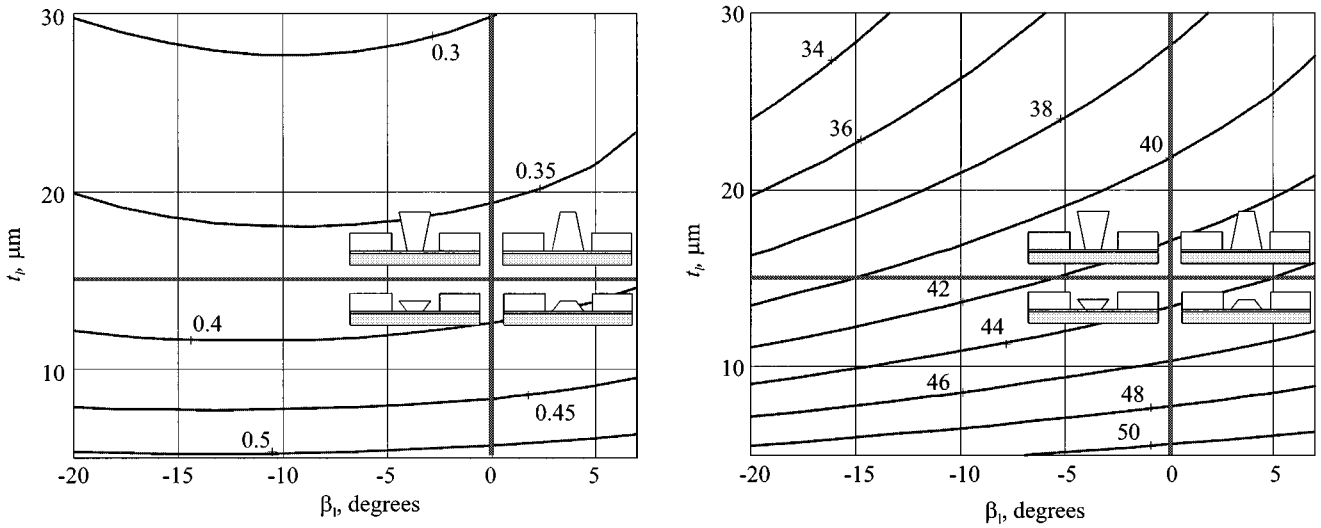

Fig. 8. Attenuation (in decibels per centimeter) and characteristic impedance (Ω) at $f = 1$ GHz of a trapezoidal CPW ($a = 4\ \mu$m, $b = 24\ \mu$m, $t_g = 15\ \mu$m, $\beta_g = 0°$) as a function of the thickness and of the edges' inclination of the central electrode t_l, β_l. The substrate is the same as in Fig. 6.

vectors $\{w_i\}$ and $\{\alpha_i\}$. The *in vacuo* characteristic parameters may be computed from (2)–(4) by replacing (5) with

$$k = \sqrt{\frac{z_{n_l} - z_1}{z_{n_l+1} - z_1}}. \tag{14}$$

For the attenuation (6), the generalized form of (7)–(10) is

$$I_{\text{line}} = 4\mathcal{I}\frac{K(k)}{\sqrt{z_{n_l+1} - z_1}} \tag{15}$$

$$P(z) = \prod_{i=1}^{n_l+n_g-1} (z - z_i)^{\theta_i - 1} \tag{16}$$

$$\gamma_z = \bigcup_{\substack{i=1 \\ i \neq n_l}}^{n_l+n_g-1} (z_i, z_{i+1}) \tag{17}$$

where

$$\theta_i = \begin{cases} 2 - \alpha_i, & \text{for } i \notin \{1, n_l, n_l+1, n_l+n_g\} \\ 1 - \alpha_i, & \text{for } i \in \{1, n_l, n_l+1, n_l+n_g\}. \end{cases} \tag{18}$$

Maps of the *in vacuo* potential distribution may be produced with the `rectmap` function of the SC toolbox. As an example, Fig. 9 shows contour plots of the potential for electrode cross sections similar to the geometries proposed in [12] and [13], and for a CPW having an almost circular central line, modeled as a 20-sided polygon.

As a numerical exercise of application for the general case, we evaluated the parameters of a CPW with rectangular ground planes as a function of the number of sides N_s of the central electrode (whose cross section represents one-quarter of a regular polygon with $4(N_s - 1)$ sides: a square is obtained for $N_s = 2$). The purpose of the exercise is to assess the effect of edge singularities of the current distribution on the line losses, which are expected to be lower in the presence of smooth electrodes. Fig. 10 shows the *in vacuo* attenuation and characteristic impedance characteristic for two cases, where either the base length a or the electrode perimeter are kept constant. It may be observed that, for all practical purposes, the asymptotic value of α_0 is already reached for $N_s = 4$, thus suggesting a strong influence of the edge singularity on the line losses in the transition from $N_s = 2$ to $N_s > 2$.

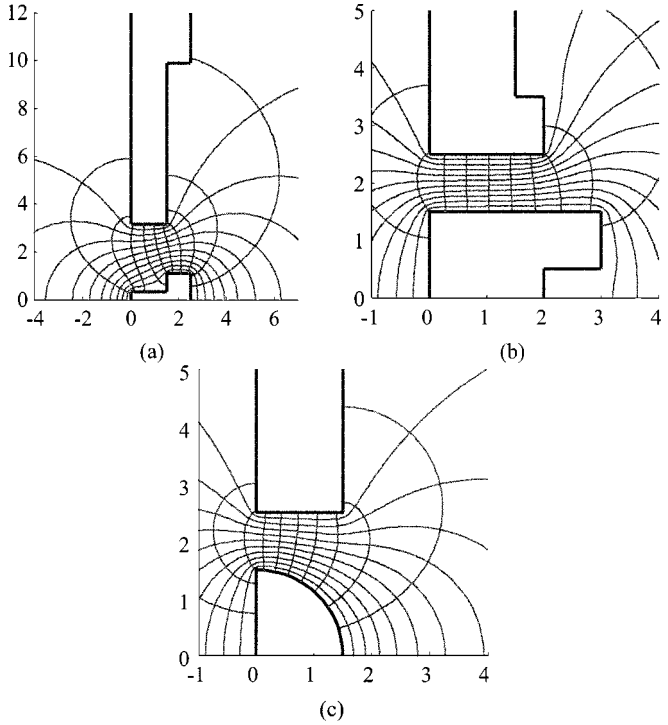

Fig. 9. Cross section and *in vacuo* potential distribution of some thick polygonal CPWs. (a) Structure proposed in [12]. (b) Generalization of the structure presented in [13]. (c) Waveguide with an almost circular central line, modeled as a 20-sided polygon.

Some comments finally are in order on the geometrical limitations of the CM approach in its present form. The above-mentioned symmetry constraints derive from the fact that the current version of the SC toolbox (2.16) can deal only with simply connected polygons (with an arbitrary number of infinite vertices). Therefore, the waveguide must have a symmetry axis either vertically, cutting the central line in its middle (as in all of the examples discussed in this paper), or horizontally. In the latter case,

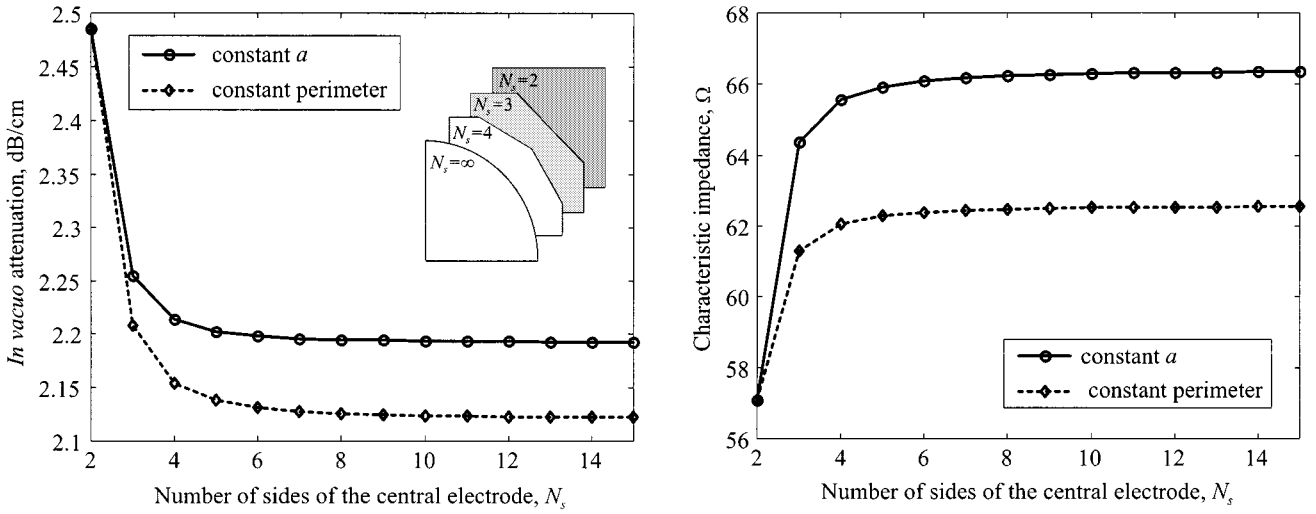

Fig. 10. *In vacuo* attenuation (in decibels per centimeter) and characteristic impedance (Ω) at $f = 1$ GHz of a CPW with $t_g = 15$ μm and distance between line and rectangular ground planes equal to 10 μm as a function of the number of sides of the central electrode. For $N_s = 2$, one has a conventional rectangular CPW with $a = t_l = t_g$; the two cases of the constant central line perimeter and constant a are compared.

which, in practice, corresponds to CPWs of rectangular shape, no limitation exists for the (vertical) line symmetry, and even multiconductor CPWs with an arbitrary number of conductors can be analyzed, as discussed in [23] and [38]. Future work may overcome, in part, the limitations of the present approach by exploiting SC transformations for doubly connected polygonal regions [39]; this could also enable one to investigate multiconductor coplanar lines of nonrectangular shape.

IV. Conclusion

The accurate computation of quasi-static parameters and skin-effect losses of (symmetric) CPWs with arbitrary cross section has been addressed as an application of the SC toolbox. The computed results are in excellent agreement with the FW FEM, while the computational efficiency of the approach enables its use within the framework of an optimization tool. A few examples of many-sided polygonal waveguides have been discussed, and the case of the trapezoidal CPW has been described in full detail, in order to provide a complete working example. The structures considered in this paper represent only a small subset of the potential applications of the SC toolbox in the domain of microwave transmission lines.

References

[1] P. Henrici, *Applied and Computational Complex Analysis. Volume 1. Power Series—Integration—Conformal Mapping—Location of Zeros*. New York: Wiley, 1974.

[2] S. Ramo, J. R. Whinnery, and T. Van Duzer, *Fields and Waves in Communication Electronics*, 3rd ed. New York: Wiley, 1994.

[3] K. J. Binns and P. J. Lawrenson, *Analysis and Computation of Electric and Magnetic Field Problems*, 2nd ed. New York: Pergamon, 1973.

[4] I. S. Gradshteyn and I. M. Ryzhik, *Tables of Integrals, Series, and Products*, 5th ed. New York: Academic, 1994.

[5] K. C. Gupta, R. Garg, and I. J. Bahl, *Microstrip Lines and Slotlines*, 2nd ed. Norwood, MA: Artech House, 1996.

[6] B. C. Wadell, *Transmission Line Design Handbook*. Norwood, MA: Artech House, 1991.

[7] W. Heinrich, "Quasi-TEM description of MMIC coplanar lines including conductor-loss effects," *IEEE Trans. Microwave Theory Tech.*, vol. 41, pp. 45–52, Jan. 1993.

[8] G. Ghione, M. Goano, and M. Pirola, "Exact conformal-mapping models for the high-frequency losses of coplanar waveguides with thick electrodes of rectangular or trapezoidal cross section," in *IEEE MTT-S Int. Microwave Symp. Dig.*, vol. 4, Anaheim, CA, June 1999, pp. 1311–1314.

[9] G. Ghione, M. Goano, G. Madonna, G. Omegna, M. Pirola, S. Bosso, D. Frassati, and A. Perasso, "Microwave modeling and characterization of thick coplanar waveguides on oxide-coated lithium niobate substrates for electro-optical applications," *IEEE Trans. Microwave Theory Tech.*, vol. 47, pp. 2287–2293, Dec. 1999.

[10] M. Seino, N. Mekada, T. Yamane, Y. Kubota, M. Doi, and T. Nakazawa, "20-GHz 3-dB-bandwidth Ti:$LiNbO_3$ Mach–Zehnder modulator," in *16th European Conf. Opt. Commun.*, Amsterdam, Holland, Sept. 1990, pp. 999–1002.

[11] G. K. Gopalakrishnan, W. K. Burns, R. W. McElhanon, C. H. Bulmer, and A. S. Greenblatt, "Performance and modeling of broad-band $LiNbO_3$ traveling wave optical intensity modulators," *J. Lightwave Technol.*, vol. 12, pp. 1807–1819, Oct. 1994.

[12] R. Madabhushi, Y. Uematsu, and M. Kitamura, "Wide-band Ti:$LiNbO_3$ optical modulators with reduced microwave attenuation," in *23rd European Conf. Opt. Commun.*, Edinburgh, Scotland, Sept. 1997, pp. 29–32.

[13] K. Noguchi, H. Miyazawa, and O. Mitomi, "40-Gbit/s Ti : $LiNbO_3$ optical modulator with a two-stage electrode," *IEICE Trans. Electron.*, vol. E81-C, pp. 1316–1320, Aug. 1998.

[14] K. Kawano, K. Noguchi, T. Kitoh, and H. Miyazawa, "A finite element method (FEM) analysis of a shielded velocity-matched Ti : $LiNbO_3$ optical modulator," *IEEE Photon. Technol. Lett.*, vol. 3, pp. 919–921, Oct. 1991.

[15] O. Mitomi, K. Noguchi, and H. Miyazawa, "Design of ultra-broad-band $LiNbO_3$ optical modulator with ridge structure," *IEEE Trans. Microwave Theory Tech.*, vol. 43, pp. 2203–2207, Sept. 1995.

[16] M. Koshiba, Y. Tsuji, and M. Nishio, "Finite-element modeling of broad-band traveling-wave optical modulators," *IEEE Trans. Microwave Theory Tech.*, vol. 47, pp. 1627–1633, Sept. 1999.

[17] H. A. Wheeler, "Formulas for the skin effect," *Proc. IRE*, vol. 30, pp. 412–424, Sept. 1942.

[18] T. A. Driscoll, "Algorithm 756: A MATLAB toolbox for Schwarz–Christoffel mapping," *ACM Trans. Math. Softw.*, vol. 22, no. 2, pp. 168–186, June 1996.

[19] ——, *Schwarz–Christoffel Toolbox User's Guide: Version 2.1*. Boulder, CO: Dep. Appl. Math., Univ. Colorado, 1999.

[20] G. H. Owyang and T. T. Wu, "The approximate parameters of slot lines and their complement," *IRE Trans. Antennas Propagat.*, vol. AP-6, pp. 49–55, Jan. 1958.

[21] G. Ghione, "A CAD-oriented analytical model for the losses of general asymmetric coplanar lines in hybrid and monolithic MICs," *IEEE Trans. Microwave Theory Tech.*, vol. 41, pp. 1499–1510, Sept. 1993.

[22] C. L. Holloway and E. F. Kuester, "A quasi-closed form expression for the conductor loss of CPW lines, with an investigation of edge shape effects," *IEEE Trans. Microwave Theory Tech.*, vol. 43, pp. 2695–2701, Dec. 1995.

[23] G. Ghione, M. Goano, and C. U. Naldi, "A CAD-oriented model for the ohmic losses of multiconductor coplanar lines in hybrid and monolithic MIC's," in *GAAS'96*, Paris, France, p. 8A2.
[24] G. Ghione and M. Goano, "A closed-form CAD-oriented model for the high-frequency conductor attenuation of symmetrical coupled coplanar waveguides," *IEEE Trans. Microwave Theory Tech.*, vol. 45, pp. 1065–1070, July 1997.
[25] ——, "The influence of ground plane width on the ohmic losses of coplanar waveguides with finite lateral ground planes," *IEEE Trans. Microwave Theory Tech.*, vol. 45, pp. 1640–1642, Sept. 1997.
[26] W.-K. Wang, R. W. Smith, and P. J. Anthony, "Full-wave analysis of coplanar waveguides for $LiNbO_3$ optical modulators by the mode-matching method considering nonideal conductors on etched buffer layers," *J. Lightwave Technol.*, vol. 13, pp. 2250–2257, Nov. 1995.
[27] R. Madabhushi, "Microwave attenuation reduction techniques for wide-band Ti:$LiNbO_3$ optical modulators," *IEICE Trans. Electron.*, vol. E81-C, pp. 1321–1327, Aug. 1998.
[28] W. Hilberg, "From approximations to exact relations for characteristic impedances," *IEEE Trans. Microwave Theory Tech.*, vol. MTT-17, pp. 259–265, May 1969.
[29] R. Piessens, E. deDoncker Kapenga, C. W. Überhuber, and D. K. Kahaner, *QUADPACK: A Subroutine Package for Automatic Integration*. Berlin, Germany: Springer-Verlag, 1983.
[30] T. A. Driscoll and S. A. Vavasis, "Numerical conformal mapping using cross-ratios and Delaunay triangulation," *SIAM J. Sci. Comput.*, vol. 19, no. 6, pp. 1783–1803, Nov. 1998.
[31] M. Koshiba, *Optical Waveguide Theory by the Finite Elements Method*. Tokyo, Japan: KTK Sci., 1992.
[32] G. Pelosi, R. Coccioli, and S. Selleri, *Quick Finite Elements for Electromagnetic Waves*. Norwood, MA: Artech House, 1998.
[33] F. A. Fernandez, Y. C. Yong, and R. D. Ettinger, "A simple adaptive mesh generator for 2-D finite element calculations," *IEEE Trans. Magn.*, vol. MAG-29, pp. 1882–1885, Mar. 1993.
[34] M. Koshiba, S. Maruyama, and K. Hirayama, "A vector finite-element method with the high-order mixed-interpolation-type triangular elements for optical waveguiding problems," *J. Lightwave Technol.*, vol. 12, pp. 495–502, Mar. 1994.
[35] Y. Tsuji and M. Koshiba, "Adaptive mesh generation for full-vectorial guided-mode and beam-propagation solutions," *IEEE J. Select. Topics Quantum Electron.*, vol. 6, pp. 163–169, Jan./Feb. 2000.
[36] R. B. Morgan, "On restarting the Arnoldi method for large nonsymmetric eigenvalue problems," *Math. Comput.*, vol. 65, no. 215, pp. 1213–1230, July 1996.
[37] R. B. Lehoucq, D. C. Sorensen, and C. Yang, *ARPACK Users' Guide: Solution of Large-Scale Eigenvalue Problems With Implicitly Restarted Arnoldi Methods*. Philadelphia, PA: SIAM, 1998.
[38] G. Ghione, "An efficient, CAD-oriented model for the characteristic parameters of multiconductor buses in high-speed digital GaAs ICs," *Analog Integrated Circuits Signal Processing*, vol. 5, no. 1, pp. 67–75, Jan. 1994.
[39] C. Hu, "Algorithm 785: A software package for computing Schwarz–Christoffel conformal transformation for doubly connected polygonal regions," *ACM Trans. Math. Softw.*, vol. 24, no. 3, pp. 317–333, Sept. 1998.
[40] M. Kobayashi and R. Terakado, "New view on an anisotropic medium and its application to transformation from anisotropic to isotropic problems," *IEEE Trans. Microwave Theory Tech.*, vol. MTT-27, pp. 769–775, Sept. 1979.

Michele Goano (M'98) received the Laurea degree and the Ph.D. in electronics engineering from the Politecnico di Torino, Turin, Italy in 1989 and 1993, respectively.

In 1994 and 1995, he was a Post-Doctoral Fellow in the Département de Génie Physique, École Polytechnique de Montréal, Montréal, QC, Canada. Since 1996, he has been a Research Assistant in the Dipartimento di Elettronica, Politecnico di Torino. He was a Visiting Scholar in the School of Electrical and Computer Engineering, Georgia Institute of Technology, Atlanta, and in the Department of Electrical and Computer Engineering, Boston University, Boston, MA. He has been engaged in modeling of semiconductor optical components and Monte Carlo simulation of quantum-well devices, and is currently involved in research on coplanar components, traveling-wave modulators, and wide-bandgap semiconductors.

Francesco Bertazzi received the Laurea degree in electronics engineering from the Politecnico di Torino, Turin, Italy in 2000, and is currently working toward the Ph.D. degree in electronics engineering at the Politecnico di Torino.

His research is focused on the application of the finite-element method to waveguiding problems.

Paolo Caravelli is currently working toward the Laurea degree in electronics engineering at the Politecnico di Torino, Turin, Italy.

His research concerns modeling and design of traveling-wave electrooptical modulators.

Giovanni Ghione (M'87-SM'94) received the Electronics Engineering degree from the Politecnico di Torino, Turin, Italy in 1981.

From 1983 to 1987, he was a Research Assistant with the Politecnico di Torino. From 1987 to 1990, he was an Associate Professor with the Politecnico di Milano, Milan, Italy. In 1990, he joined the University of Catania, Catania, Italy, as a Full Professor of electronics. Since 1991, he has been a Full Professor on the II Faculty of Engineering, Politecnico di Torino. Since 1981, he has been engaged in Italian and European research projects (ESPRIT 255, COSMIC, and MANPOWER) in the field of active and passive microwave computer-aided design (CAD). His current research interests concern the physics-based simulation of active microwave and opto-electronic devices, with particular attention to noise modeling, thermal modeling, and active device optimization. His research interests also include several topics in computational electromagnetics, including coplanar component analysis. He has authored or coauthored over 150 papers and book chapters in the above fields.

Prof. Ghione is member of the Associazione Elettrotecnica Italiana (AEI). He is an Editorial Board member of the IEEE TRANSACTIONS ON MICROWAVE THEORY AND TECHNIQUES.

Tobin A. Driscoll received the B.S. degrees in both mathematics and physics from the Pennsylvania State University, University Park, in 1991, and the Ph.D. degree in applied mathematics from Cornell University, Ithaca, NY, in 1996.

In 2000, he joined the faculty of the Department of Mathematical Sciences, University of Delaware, Newark, where he studies numerical methods for differential equations.

Dr. Driscoll is a member of the Society for Applied and Industrial Mathematics.